X-ray Absorption Spectroscopy of a New Zinc Site in the Fur Protein from *Escherichia coli*†

Lilian Jacquamet,‡ Daniel Aberdam,§ Annie Adrait,‡ Jean-Louis Hazemann,§,|| Jean-Marc Latour,*,‡ and Isabelle Michaud-Soret*,‡

Département de Recherche Fondamentale sur la Matière Condensée, Service de Chimie Inorganique et Biologique, Laboratoire de Chimie de Coordination (Unité de Recherche Associée au CNRS No.1194), CEA-Grenoble, 38054 Grenoble Cedex 9, France, Laboratoire de Cristallographie, UPR 5031 CNRS, BP 166, 38042 Grenoble Cedex 9, France, and Laboratoire de Géophysique Interne et Tectonophysique, UMR 5559, UJF-CNRS, BP 53, 38041 Grenoble Cedex 09, France

Received August 27, 1997; Revised Manuscript Received December 1, 1997

ABSTRACT: The zinc K-edge X-ray absorption spectra of the Fur (ferric uptake regulation) protein isolated from *Escherichia coli* have been analyzed in frozen solution to determine details of the zinc coordination. The spectra of apoFur and of the cobalt-substituted protein have been analyzed and compared in order to see the influence of the cobalt incorporation on the geometry of the zinc site. EXAFS analysis gave for both samples (apoFur and CoFur) a tetrahedral environment for the zinc atom with two sulfur donor ligands at a distance of 2.3 Å from the zinc and two N/O donor ligands at 2.0 Å. The two sulfur donor ligands are probably two of the four cysteines present in each Fur monomer and could be Cys92 and Cys95, which are known from mutagenesis studies to be essential for Fur activity [Coy, M., Doyle, C., Besser, J., and Neilands, J. B. (1994) *BioMetals 7*, 292−298]. The distances obtained from our fits were always too short to be compatible with penta or hexa coordination. The typical pattern observed for the Fourier transform of the EXAFS oscillations suggests the presence of at least one imidazole ligand. The XANES of these two forms of the protein are similar but significantly different. This suggests a change of the conformation of the zinc site upon cobalt incorporation. The present study provides the first unambiguous evidence for the presence of a structural zinc site in the Fur protein from *Escherichia coli*.

The control of the intracellular iron concentration in Gram-negative bacteria such as *Escherichia coli* is done at the level of the iron uptake inside the cell (*2*, *3*). In several Gram-negative bacteria such as *E. coli*, the regulation of various bacterial genes related to the iron uptake is effected by Fur[1] (for ferric uptake regulation), a metalloregulatory protein (*4*, *5*). Fur has been proposed to bind iron, in vivo, as a corepressor and then to act as a negative regulator via sequence-specific protein−DNA interactions at the promoter regions of Fur-regulated genes (*4*, *6*−*8*). Bagg et al. (*4*) described that all first row divalent metal ions could, with varying degrees of efficiency, allow Fur to bind the operator. In vitro, the protein can be activated by Mn^{2+}, Fe^{2+}, Co^{2+}, Cu^{2+}, Zn^{2+}, and Cd^{2+} but only by Mn^{2+}, Fe^{2+} and Co^{2+} in vivo (*4*, *9*).

The affinity constants of Fur for these dications vary from 10 to 100 μM (*4*). Since they are able to activate the protein, these dications probably bind it at the same site as the physiological co-repressor Fe^{2+}. Furthermore, it has recently been shown that the type of interaction between Fur and DNA is unique (*10*). The DNA binding site is proposed to be in the N-terminal part of the protein. The C-terminal domain is proposed to contain the dimerization site and probably the metal binding site(s) (*7*, *8*).

A few spectroscopic studies of Fur have been described using NMR, UV−visible, and EPR spectroscopies (*11*, *12*). Hamed et al. (*12*, *13*) described electronic absorption and EPR studies of the protein substituted with Mn^{2+}, Fe^{2+}, Co^{2+}, and Cu^{2+}; for these metals, they found dissociation constant (K_d) values of 85, 55, 36, and 10 mM for the metal−Fur complexes, respectively. They described only one metal binding site per monomer of Fur for iron or manganese, with an octahedral environment of the iron (from Mössbauer study (*13*)). From UV−visible studies, they also found a tetrahedral environment for the Co site with coordinating sulfur atoms and up to six binding sites per monomer. An EPR study of Fur substituted with copper showed the existence of two different environments, a major one axially distorted with N/O donors corresponding to a type 2 center ($A = 156$ G) and a minor one of type 1 ($A = 75$ G) tetrahedrally distorted with sulfur donors (*12*). Unfortunately some of these results are confusing and could not be reproduced in

† This work was supported by a grant (E 90010 00 00) from the 'Région Rhône-Alpes'.

* Authors to whom correspondence should be addressed: fax: (33) 4 76 88 50 90; e-mail: latour@drfmc.ceng.cea.fr and michaud@drfmc.ceng.cea.fr.

‡ Laboratoire de Chimie de Coordination.

§ Laboratoire de Cristallographie.

|| Laboratoire de Géophysique Interne et Tectonophysique.

[1] Abbreviations: Fur, ferric uptake regulation; XAS, X-ray absorption spectroscopy; EXAFS, extended X-ray absorption fine structure; XANES, X-ray absorption near-edge structure; EPR, electron paramagnetic resonance; ICP−AES, inductive coupling plasma−atomic emission spectroscopy; EDTA, ethylenediaminotetraacetic acid; PMSF, phenylmethanesulfonyl fluoride; MOPS, 4-morpholinepropanesulfonic acid; Tris, tris(hydroxymethyl)aminomethane; ESRF, European Synchrotron Radiation Facility; LURE, Laboratoire de l'Utilization du Rayonnement Electromagnétique; DESY, Deutsches Elektronen-Synchrotron.

S0006-2960(97)02134-X CCC: $15.00
Published on Web 02/06/1998

Table 1: Experimental Conditions for the Samples Studied

no.	ref compounds	Zn environment	synchrotron	temp (K)	energy E_0 of the edge (eV)	ref
1	(hexakis-imidazole) zinc(II) dichloride	N_6	LURE	77	9665.0	(*23*)
			ESRF	298		
2	2,6-bis((mercaptophenyl)amino(1-ethyl))pyridine zinc(II)	N_3S_2	LURE	77	9663.0	(*20*)
3	2,6-bis(mercaptophenyl)imino(1-ethyl))pyridine	N_3S_2	LURE	77	9663.0	(*21*)
4	tetrakis(2-methylimidazole)zinc(II) perchlorate	N_4	LURE	77	9663.0	(*24*)
5	zinc(II) ethylxanthate	S_4	DESY	10	9663.1	(*18*)
6	tetrakisimidazole zinc(II) perchlorate	N_4	DESY	10	9663.1	(*18*)
7	sphalerite	S_4	LURE	298	9663.0	(*19*)
8	zinc oxide	O_4	DESY	10	9663.3	(*18*)
9	2,3-bis((mercaptophenyl)amino)butane zinc(II)	N_2S_2	LURE	77	9661.0	(*22*)
10	2,3-bis((mercaptophenyl)amino)butadiimine zinc(II)	N_2S_2	LURE	77	9663.0	
11	(bisimidazole) zinc(II) dichloride	N_2Cl_2	LURE	77	9663.0	(*25*)

protein samples	Zn environment	synchrotron	temp (K)	energy E_0 of the edge (eV)	ref
apoFur	?	ESRF	77	9662.1	this work
CoFur	?	ESRF	77	9663.1	this work

our hands. In particular, we found for the cobalt-substituted protein a well-defined penta- or hexa-coordinated monomer binding site containing N/O donor ligands (unpublished results). Furthermore, since it activates the protein, the cobalt should bind at the same site as manganese and iron. Therefore, it appears that the environment of the metals is still largely unknown even if histidines and cysteines have been postulated as ligands (*1*, *11*−*13*).

Histidines and cysteines are well conserved in the sequences of the Fur proteins described in the literature (*8*, and as seen from sequence alignments of the sequences of the Fur proteins found in the GenBank Database). Mutation studies on several of the 12 histidines present in the sequence give a partial loss of activity and mutation of two of the four cysteines (Cys92 and Cys95) to serine results in a complete loss of activity (*1*). The four cysteines are grouped in two pairs (C92-X2-C95 and C134-X4-C139) with a spacing reminiscent of the one observed in the sequences of zinc finger containing proteins (*14*). Furthermore, Fur also has a tight-binding zinc site, since we found that apoFur and CoFur contain 0.5−0.8 Zn atom per monomer as measured by ICP analysis (*15*). However, the environment of this zinc binding site and the amino acids bound to the zinc are still unknown. In order to further investigate the structure of this new zinc binding site in Fur, we have undertaken an X-ray absorption spectroscopy (XAS) study of Fur-bound zinc. Since the Zn^{2+} ion has a d^{10} electronic structure, XAS is the only spectroscopic method that can give direct information on the ligands of a zinc site without resorting to metal substitution or site-directed mutagenesis experiments. In particular, a XAS study can unambiguously identify sulfur coordination, thereby assessing cysteine/methionine ligation. In addition, the presence of imidazole ligands in the metal coordination sphere gives a characteristic pattern in the EXAFS spectra (*16*, *17*). Our goal was to identify the type of ligands of the zinc ion and to probe if this newly found zinc site has an environment typical of a structural (cysteine-containing) zinc environment (*14*).

We present in this paper the zinc K-edge X-ray absorption spectra analysis of Fur, the ferric uptake regulation protein isolated from *Escherichia coli* in frozen solution. ApoFur and CoFur have been characterized and analyzed using XAS in order to determine the local structure of the zinc site and to evaluate the influence of cobalt incorporation on its geometry. XAS analysis of the two samples for both apoFur and CoFur points to a tetrahedral environment for the zinc atom with two sulfur donor ligands and two N/O donor ligands, one of them at least being an histidine.

EXPERIMENTAL PROCEDURES

Reference Compounds

The reference compounds have been selected for their chemical environment as close as possible from the one postulated for the protein. Table 1 reports the list of compounds and the experimental conditions for the XAS experiments. The absorption spectra of compounds **5**, **6**, and **8** have been obtained and studied by H.-F. Nolting in 1989 (*18*) and kindly communicated to us. Compound **7** (*19*) and compounds **2**, **3**, **9**, and **10** (*20*−*22*) were kindly provided by G. Sarret and I. Artaud, respectively. Compounds **1**, **4**, and **11** were synthesized according to published procedures (*23*−*25*). In the case of compound **4**, the crystal structure differed from the one previously described and has been solved by X-ray diffraction techniques: Monoclinic space group Cc, a = 15.8728(8) Å, b = 16.2549(8) Å, c = 11.4501(5) Å, β = 121.328(1)°, V = 2523.5(2) Å^3; Zn−N bond distances: 1.978, 1.988, 1.996, and 2.016 Å.

Preparation of the Protein Samples

Overproduction and Purification of Fur. The T7 RNA polymerase/promoter system was used to overproduce the Fur protein from *Escherichia coli* as previously described (*26*). The Fur protein was purified as previously described (*27*) but with some modifications (*15*). The first modification concerns the addition of trypsin−chymotrypsin inhibitors (from Sigma) at 10 mg L^{-1} together with EDTA at 20 mM, PMSF at 1.38 mM, and pepstatin at 5.8 mM in the extraction buffer (0.1 M MOPS buffer at pH = 8 containing 10% w/v sucrose and 10% v/v glycerol) in order to avoid proteolysis. The second modification is the addition of another step of purification after the chelating zinc iminodiacetate column using a gel filtration on Superdex 75 (Pharmacia) in 0.1 M Tris-HCl at pH = 8 (5 °C) containing 0.1 M KCl. Before this second step of purification, a treatment with 20 mM EDTA for 30 min at 4 °C was performed on the regrouped fractions collected from the chelating column. A precipita-

tion at 80% ammonium sulfate saturation was run overnight before solubilization of the protein in 2 mL of 0.1 M Tris-HCl at pH = 8 (5 °C) containing 0.1 M KCl with 10% v/v glycerol and loading on the gel filtration column. The samples collected from the gel filtration were concentrated, and 10% v/v glycerol was added. They are then stored in liquid nitrogen and constitute the apoFur samples.

Protein Concentration Measurements. Protein concentrations were determined spectrophotometrically using an absorption coefficient at 275 nm of 0.4 mg^{-1} mL cm^{-1} (*27*) for one monomer of pure apoFur.

Metal Incorporation. Cobalt incorporation in apoFur was followed by the appearance of a band at ca. 550 nm ($\epsilon = 70$ M^{-1} cm^{-1}) in the UV−visible spectrum (unpublished results) recorded on a Lambda 9 Perkin-Elmer spectrophotometer. Metal (Co and Zn) quantifications were obtained by analysis using inductive coupling plasma−atomic emission spectroscopy (ICP−AES) on a Fisons 'maxim type' analyzer. Low-temperature EPR spectra were recorded on a Varian E109 spectrometer equipped with an Oxford Instruments ESR-9 continuous-flow helium cryostat.

XAS Experiments

XAS Samples Preparation. Two types of samples have been prepared, the first one called apoFur and the second containing a stoichiometric amount of cobalt called CoFur. For the latter, the buffer had been exchanged with the following buffer: 0.1 M phosphate, pH = 8, and 10% v/v glycerol. The 10% v/v glycerol was always added to the samples in order to avoid the presence of diffraction signals in the XAS spectra. The samples were brought to 100 μL by concentration on Centricon 10 (Amicon). The final concentration in protein was 5.3 and 3.3 mM for the apoFur and the CoFur samples, respectively. The metal concentrations from the ICP analysis were 4.2 mM in zinc in the apoFur and 2.6 mM in zinc and 2.8 mM in cobalt in the CoFur sample.

XAS Measurements. XANES and EXAFS spectra of reference compounds **1**−**4**, **7**, and **9**−**11** (see Table 1 and Figure 1) were recorded in transmission mode at 77 K on the XAS 13 beamline at the 'Laboratoire de l'Utilisation du Rayonnement Electromagnétique' (LURE, Orsay) equipped with a channel-cut monochromator of Si(311). The critical energy of a bending magnet at LURE is around 4 keV, so the contribution of the third harmonic can be neglected. Energy resolution of the monochromator was around 1.0 eV. Energy calibration was accomplished using Zn foil as an internal standard and assigning the energy of the maximum of the foil absorption spectra as 9669 eV.

Spectra of compounds **5**, **6**, and **8** were kindly provided by H.-F. Nolting. XAS measurements were performed at Deutsches Elektronen-Synchrotron (DESY) and were described in ref *18*.

The spectra of **1** and of the protein samples were recorded at the European Synchrotron Research Facility (ESRF, Grenoble) on the Collaborative Research Group IF BM 32 beamline equipped with a double-crystal monochromator of Si(111). The harmonics rejection was done with the use of a nickel-coated mirror first and a double-platinum-coated mirror second. Energy resolution of the monochromator was 2.0 eV. Energy calibration was accomplished by assigning the energy of the maximum of the spectrum derivative of **1** as 9665.0 eV; the value was determined at LURE for the same compound. The two protein samples have been studied at the Zn K-edge from 9500 to 10 400 eV in fluorescence mode at 77 K and compound **1** in transmission mode at room temperature. The K_α fluorescence was measured with a solid Canberra detector containing five elements. The counting time varied from 3 s in the pre-edge region to 10 s at 14 $Å^{-1}$ for a total integration time of 35 min/scan. The sample cell was designed specifically for fluorescence measurements. Its shape was calculated in order to optimize the detection for the beam size (0.3 × 0.3 mm^2 at full-width half-maxima). It was a gold-coated copper cell in order to avoid copper fluorescence and copper contamination of the samples.

Data Analysis. The analysis was made in harmonic approximation with plane waves (*28*) using a program developed by D. Aberdam (*29*). Each scan was first normalized by the height of the absorption jump at the edge, and then the average of six scans was calculated to obtain the final spectrum. The extraction of EXAFS oscillations from the final spectra was accomplished using the procedure described by D. Aberdam in ref *29*. The data were then converted in the *k*-space according to:

$$k = \sqrt{\frac{2m_e(E - E_0)}{\hbar^2}} \qquad (1)$$

E_0 values are reported in Table 1 and have been chosen at the maximum of the edge derivative. The resultant EXAFS data were weighted by k^3 and Fourier transformed over the region $k = 2-12$ $Å^{-1}$ using an apodization window of Kaiser with plateau (*29*). The curve fitting was then realized on the Fourier-filtered first shell between 1.1 and 2.5 Å weighted by the statistical noise. The noise was estimated in the $k^3\chi(k)$ data by computing the difference between the raw experimental EXAFS signal and the filtered one. The statistical error is taken as the mean root square value of this difference.

As a measure of the sample integrity, we compared the XAS spectra measured for the first and the last scan of each sample. No spectral changes were observed over the course of the data collection, indicating that no change is occurring in the metal center.

Extraction of the Structural Parameters. In isotropic conditions (without polarization effect) and for a Gaussian distribution of distances, the EXAFS data can be described by

$$k\chi(k) = S_0^2 \sum_i \frac{N_i}{R_i^2} \left| f_i(k) \right| e^{-2\sigma_i^2 k^2} e^{-2R_i/\lambda(k)} \sin(2kR_i + \phi_{ij}(k)) \qquad (2)$$

In eq 2, N_i is the number of scatterers at distance R_i from the absorber in shell *i*; $f_i(k)$ and $\phi_{ij}(k)$ are the backscattering amplitude and the total phase-shift of the absorber−scatterer pairs, respectively; σ_i^2 contains a thermal agitation component (Debye−Waller type) and a standard deviation component of the distance distribution (Gaussian approximation); λ represents the mean free path, $\lambda(k)$, of the ejected photoelectron; and S_0^2 is the reduction factor.

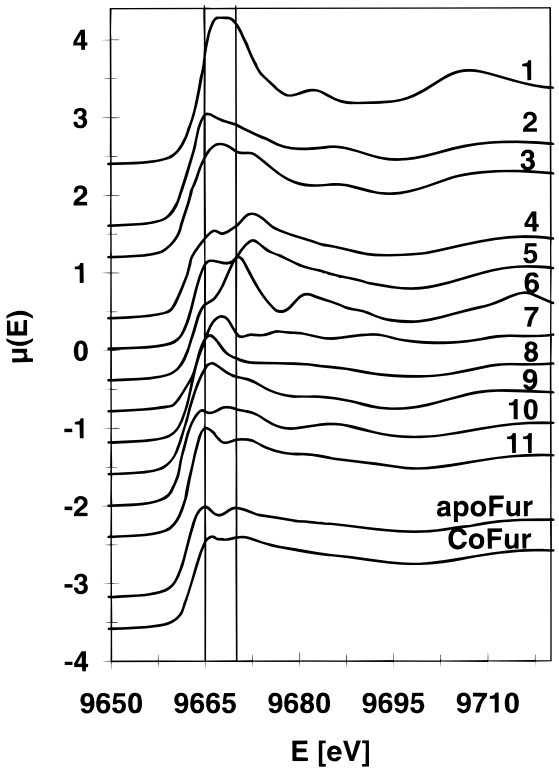

FIGURE 1: XANES spectra of the reference compounds and of the protein samples.

Ab initio parameters for amplitude, $f_i(k)$, and phase, $\phi_{ij}(k)$, and mean free path were calculated using the program FEFF 6.01 (*30*, *31*). Then eq 2 is rewritten as:

$$k\chi(k) = S_0{}^2 \sum_i \frac{N_i}{R_i{}^2} \left| F_{\mathrm{eff}_i}(k,R_i) \right| \mathrm{e}^{-2\sigma_i{}^2 k^2} \sin(2kR_i + \phi_{ij}(k, R_i)) \quad (3)$$

In metalloproteins, the metal coordination sphere contains oxygen, nitrogen, or sulfur donor ligands. Therefore calculations have been performed for a single absorber−scatterer pair Zn−O at 2.00 Å distance, for a single Zn−N interaction at 2.05 Å and a single Zn−S interaction at 2.35 Å (*32*).

The Fourier-filtered first shell was fitted to eq 3 using a nonlinear least-squares algorithm with a program developed by D. Aberdam (*29*). The structural parameters to be determined are for each sample: N_i, R_i, and $\sigma_i{}^2$.

The reduction factor $S_0{}^2$ and the energy shift ΔE_0 (shift in E_0 from the initial value) were calibrated by fitting model compounds **4**−**8**, which contain homogeneous environments (O_4, N_4, and S_4) and whose X-ray structure were known (see Table 1). N_i was held fixed and R_i and $\sigma_i{}^2$ were optimized. The optimal values obtained were $S_0{}^2 = 0.85$ and $\Delta E_0 = 4$ eV for the absorber−scatterer pairs, Zn−O, Zn−N, and Zn−S.

To check the validity of parameters ΔE_0 and $S_0{}^2$ calibrated from homogeneous references, they were held fixed at their optimal values to extract the structural parameters for compounds **2**, **3**, and **9**−**11**, which have a mixed environment of nitrogen and sulfur around the zinc ion. For each compound, the best fit obtained gave the number of nitrogen and sulfur atoms coordinated to the zinc ion. The differences between the bond lengths determined using this method and the ones deduced from the crystallographic data were less than 2×10^{-2} Å for Zn−N as well as for Zn−S.

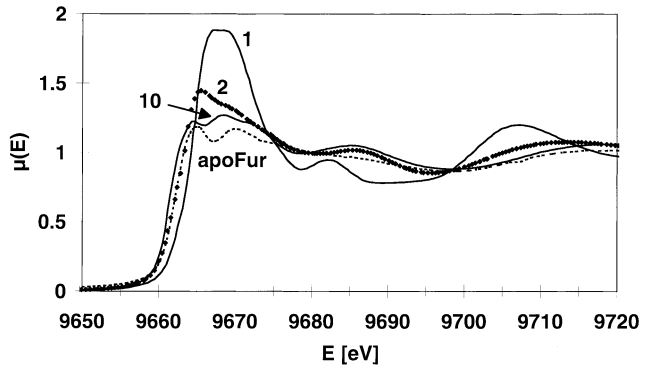

FIGURE 2: XANES spectra of **1**, **2**, and **10** and of the apoFur.

Consequently, for protein samples, ΔE_0 and $S_0{}^2$ were held fixed at the calibrated values, and the three parameters N_i, R_i, and $\sigma_i{}^2$ were deduced for each shell. Since N_i and $\sigma_i{}^2$ are strongly correlated, N_i was held fixed to chemically reasonable integer values and only R_i and $\sigma_i{}^2$ are optimized.

RESULTS

XANES. The shape and the intensity of the XANES spectra are very sensitive to the electronic structure and the chemical nature of the ligands and to the geometry of the zinc environment. Therefore, a qualitative study of a wealth of structurally characterized reference compounds was undertaken to derive structural information from the proteins XANES spectra.

XANES of the Reference Compounds. The XANES spectra of the reference compounds shown in Figure 1 illustrate the high sensitivity of XANES to the electronic structure, the chemical nature, and the geometry of the metal site.

The intensity of the so-called white line which is related to the 1s → 4p transition is dependent on the zinc coordination (*33*). The increase in coordination number from 4 to 5 and 6 could be generally associated to the increase of the white line intensity (see Figure 2). For **1**, which has an octahedral geometry, the white line has the highest intensity and the edge energy E_0 is 2 eV higher than the energy measured for the penta- or tetra-coordinated complexes (see Table 1). An intense white line is always associated to the penta-coordinated compounds. For the tetra-coordinated complexes, the white line varies in intensity depending on the nature of the complexes, but most of the time it is weaker than for the penta-coordinated species.

The intensity of the second XANES peak varies also with the chemical environment of the zinc ion as we observed with the change from ZnO_4 to $ZnIm_4$, and to ZnS_4. For a coordination sphere constituted exclusively of light atoms (N or O), the second peak is more intense than the white line. On the contrary for a sulfur environment, the second peak almost disappears. When the zinc environment comprises elements from first and second row as in **9**−**11**, the second peak may become almost as intense as the white line.

Comparison of **9** and **10** shows that the geometry around the metal can also strongly modify the shape of the XANES. Indeed a shift in the energy of the edge of −2 eV is noted between the imine complex **10** and its amine counterpart **9**.

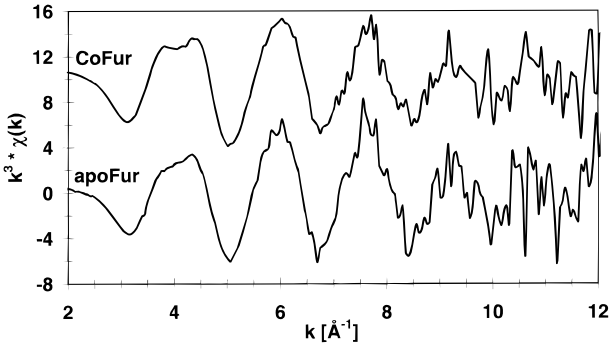

FIGURE 3: EXAFS spectra of apoFur and CoFur.

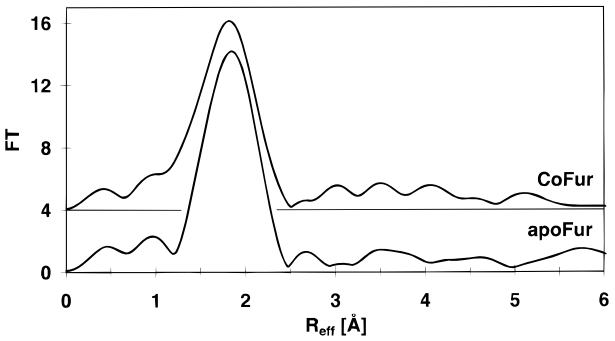

FIGURE 4: Fourier transform of apoFur and CoFur.

The imine ligand of **10** probably imposes a square planar geometry while a tetrahedral geometry is obtained upon reduction in amine as in compound **9**. The edge energy shift is likely to originate from this change in geometry from square planar to distorted tetrahedral geometry. Nevertheless, it must be kept in mind that reduction of the imine increases the electron density on nitrogen between **10** and **9** what can also influence the XANES in that case. These results confirm that a qualitative analysis of the XANES could give information on the geometry and on the nature of a zinc binding site of unknown structure as the one in Fur.

XANES of Fur Samples. The normalized XANES spectra of apoFur and CoFur are shown at the bottom of Figure 1. Their shapes are similar but not strictly identical, and the main difference is a shift of the edge energy of +1 eV when Co^{2+} is incorporated into the protein (see Table 1). Comparison of the XANES spectra of the two Fur samples with those of the reference compounds suggests that the zinc site in the protein is probably tetrahedral with a mixed environment of N/O and S, since the white line is small and there is clearly two XANES peaks (see Figure 2). The similarity of the Fur derivatives with **11** possessing a N_2Cl_2 environment is noteworthy in this respect.

EXAFS of Fur Samples. The EXAFS spectra of apoFur and CoFur are shown in Figure 3. The two spectra look almost identical. This suggests that the zinc ion has the same chemical environment in apoFur and CoFur. The first EXAFS oscillation contains a shoulder between 3 and 5 $Å^{-1}$, which is characteristic of the presence of a imidazole group(s) as ligand(s) of the metal (*34*). This shoulder is bigger for CoFur than for apoFur. The Fourier-transformed spectrum of CoFur shown in Figure 4 has a major signal at R_{eff} (uncorrected from the phase shift) $\approx$ 1.85 Å and three secondary signals at $R_{eff} \geq 3$ Å. These three weak signals originate in the scattering from the outer atoms of imidazole group(s) bound to the metal and contain multiple scattering contributions (*35*). These secondary signals do not appear clearly in the Fourier-transformed spectrum of apoFur, but a slight distortion of the zinc environment in apoFur, such as the one evidenced in the XANES spectra, can decrease drastically the intensity of signals of the outer atoms.

Table 2: Structural Parameters for the Fits Concerning apoFur and CoFur

neighbors	R_N (Å)	$\sigma_N^2 \times 10^3$	R_S (Å)	$\sigma_S^2 \times 10^3$	$I \times 10^2$ [a]
		apoFUR			
2 N	2.07	6.8 (7)			3.15
3 S			2.31	6.2 (2)	
3 N	2.06	5.7 (4)			3.99
2 S			2.32	3.1 (2)	
2 N	2.05	1.1 (2)			1.61
2 S			2.32	2.0 (1)	
		CoFUR			
2 N	2.05	10.6(10)			3.64
3 S			2.30	7.6 (2)	
3 N	2.04	9.2 (5)			2.45
2 S			2.31	4.6 (2)	
1 N	2.03	2.4 (6)			4.96
3 S			2.31	6.5 (2)	
2 N	2.03	4.1 (3)			2.26
2 S			2.31	3.7 (1)	
3 N	2.05	4.2 (3)			4.52
1 S			2.32	0 (2)	

[a] $$I = \frac{\sum_i \frac{(k^3\chi(k)_{exp} - k^3\chi(k)_{cal})}{\sigma_i^2}}{\sqrt{\chi_{exp}^2}}$$

with σ_i^2 as the term related to the noise at each point.

The absence of a large detectable secondary signal in the Fourier transform of CoFur between 1.9 and 3.5 Å suggests the absence of interaction between the zinc ion and another metal in the protein, neither Co^{2+} which is in the Fe^{2+} site nor the Zn^{2+} present in the other monomer. The same conclusion can be drawn for apoFur. In conclusion, the zinc ion found in Fur seems to occupy a mononuclear site.

The structural parameters deduced from analysis of the spectra are summarized in Table 2. Coordinations 6, 5, and 4 have been successively tested for the apoFur and the CoFur data. In a first step, the data have been fitted with sulfur atoms and nitrogens as light atoms. All N/S combinations have been considered: N_n, S_n, and $N_{n-x}S_x$ with $1 < x < n$ ($n = 6, 5, 4$). The refinements of the Fourier-filtered first shell always suggest the presence of a mixed environment of sulfur and nitrogen atoms. In every case, the hexacoordination can be ruled out because of the strong divergence between fits and experimental data (not shown). The fits and the experimental points are never in phase on the whole *k* domain studied and the amplitude of the fits are much larger than

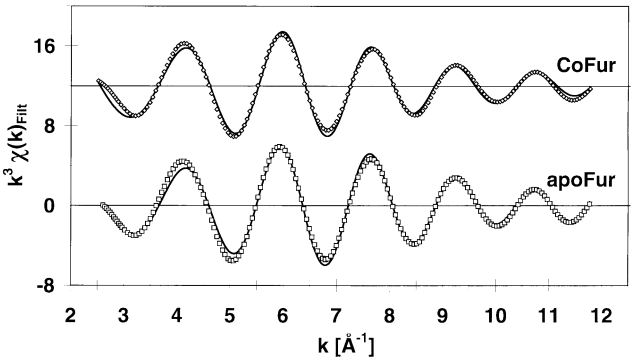

FIGURE 5: Fourier-filtered first shell of apoFur (□) and CoFur (◊) and corresponding fits (—) for a N_2S_2 environment.

the experimental ones. In the case of pentacoordination, only the N_2S_3 and N_3S_2 environments give fits with acceptable physical parameters (see Table 2).

For apoFur, the N_2S_3 and N_3S_2 environments can be eliminated because they have higher *I* fit indexes than the tetra-coordinated environments. The NS_3 and N_3S environments can be excluded because they give fits with unacceptable physical parameters. Therefore the best fit for apoFur (see Figure 5) suggests a tetrahedral environment with two nitrogen atoms at a 2.05 Å distance of the zinc and two sulfur atoms at 2.32 Å of the zinc.

In the case of CoFur, the N_2S_3, NS_3, and N_3S environments must be excluded because of their high *I* values, twice larger than the best one obtained for the tetra-coordinated N_2S_2 environment. On the other hand, the N_3S_2 environment gives an *I* value comparable to the N_2S_2 environment. However the σ_N^2 for the former is twice that of the latter and far too large compared to the values obtained for the model compounds, which leads us to reject also the N_3S_2 environment. Therefore, as in apoFur the best fit gives a N_2S_2 environment (see Figure 5), which is constituted of two nitrogen atoms at 2.03 Å and two sulfur atoms at 2.31 Å.

All fits have also been performed with oxygen in place of nitrogen atoms, and for both samples the results were similar. Not unexpectedly, the Zn−O distances were 0.03 Å smaller than the Zn−N distances previously obtained due to the larger phase shift for oxygen relative to nitrogen. The σ^2 values were larger for CoFur than for apoFur, suggesting a broader distribution of the metal−donor atom distances in CoFur.

DISCUSSION

The fits of the EXAFS data establish firmly a mixed environment of light atoms (N or O) and sulfur atoms bound to the zinc. The chemical environment seems identical in both protein samples with two N/O light atoms and two S atoms. However, the distances of the first shell atoms to the zinc are shorter in CoFur with Zn−N/O at 2.03 Å and Zn−S at 2.31 Å as compared to apoFur with Zn−N/O at 2.05 Å and Zn−S at 2.32 Å. These differences are quite small and within the usual uncertainty of EXAFS determined bond distances. However, it is noteworthy that fitting the apoFur data with CoFur Zn−N and Zn−S distances results in a significantly higher *I* value (3.87 vs 1.61) and a visible mismatch. Fitting the CoFur data with apoFur distances produces the same discrepancy. It is well documented that metal incorporation induces a conformational change of the protein (*7*). Therefore, it is possible that the structural change of the zinc site detected here be associated to this conformational change. Only a crystal structure determination will prove this point.

The distances obtained by fit are in agreement with a tetracoordinated environment. Indeed the structural data of penta- and hexa-coordinated zinc complexes containing both N and S atoms in their coordination sphere registered in the Cambridge Structural Database have been examined. It shows that the Zn−N and Zn−S distances are respectively longer than 2.10 and 2.45 Å for the former and 2.14 and 2.60 Å for the latter (see Supporting Information).

The sulfur ligands found in the EXAFS fit are probably cysteines since the Zn−S distances (2.3 Å) are in perfect accordance with Zn−S distances found in the literature for sulfur atoms from zinc bound cysteine molecules (*36*). These distances are too small to involve methionine binding.

Concerning the light atoms, the shoulder observed between 3 and 5 Å^{-1} in the EXAFS of CoFur as well as the presence of secondary signals in the Fourier transform between 3 and 4 Å are a clear signature of the presence of imidazole group(s) from histidine(s). So the EXAFS data identify the presence of at least one histidine as zinc ligand in CoFur. The other light atom ligands can possibly be a carboxylate as well as a water molecule or a histidine. The results are not as clear for apoFur because of the noise in the EXAFS data; however, both the analysis of the XANES and the fit of the EXAFS suggest a similar metal binding site in CoFur and apoFur.

The possibility of the presence of another metal in the zinc environment as well in apoFur (binuclear zinc site) as in CoFur (binuclear Zn−Co site) may be ruled out owing to the absence of any intense signal between 3 and 4 Å in the Fourier transform. Nevertheless, this hypothesis cannot be completely excluded since the signal due to the presence of another metal can be attenuated or even offset by destructive interferences of metal−metal and metal−light atoms scattering at similar distances (*37, 38*).

The comparison of the XANES part of the absorption spectra of the Fur samples with that of the model compounds is quite informative. The low intensity of the white line in apoFur and CoFur suggests a tetrahedral environment around the zinc ion. Furthermore the similar intensities of the two XANES peaks are in accordance with a mixture of light atoms (N/O) and sulfur atoms. The shape of the XANES spectra resembles the one observed for **6** (N_2Cl_2 environment) as well as those described for the transcription factor TFIIIA (*34*) and for the cobalamin-independent methionine synthase (*39*) that both contain a N_2S_2 environment around the zinc.

The modification of the XANES spectra upon cobalt incorporation in Fur is quite small, suggesting only a small change in the geometry of the zinc binding site. The +1 eV shift in the edge energy observed upon cobalt fixation confirms the assumption of a small change in the geometry of the zinc site since a comparable shift has been observed between those of **9** and **10**. Finally, the XANES data of apoFur are more structured than those of CoFur, suggesting a more distorted site in CoFur than in apoFur. Therefore it appears that cobalt incorporation at the iron(II) site probably induces a distortion of the Zn tetrahedral site without changing its ligands. EXAFS data support such a conformational change induced by cobalt incorporation. Indeed

small changes in the Zn−N and Zn−S distances are observed, and more importantly, the σ^2 values are larger for CoFur than for apoFur. The latter feature reflects a larger distance distribution in CoFur in agreement with a stronger distortion of the zinc site.

This conformational change is consistent with the observation that metal ligation activates Fur through a conformational modification. In 1991, Coy et al. (*7*) described an increase of the sensitivity of Fur to proteases such as trypsin upon metal addition and suggested that the access to the protease site (in the N-terminal part of the protein) was facilitated in the presence of metal. These results are also in accordance with the results recently published by Stojiljkovic et al. (*8*), which prove that the N-terminal part of the protein is responsible for the specific interaction of Fur with DNA. These authors suggest that the metal binding site is in the C-terminal half sequence of the protein and that a change of conformation upon metal ligation would be transmitted through the tertiary structure to the N-terminal DNA binding site.

Two main roles have been assigned to biological zinc sites. Taking advantage of its redox inertness and acidic properties, zinc enzymes often assume hydrolytic functions. In such enzymes the coordination sphere of catalytic zinc sites comprise ligands such as carboxylates or a solvent molecule susceptible of being deprotonated (*40*). On the other hand, the zinc ion may be involved in maintaining a tertiary structure conformation, such as amino acid loops in zinc finger domains (*14*, *41*). Many proteins containing such structural zinc sites interact with DNA in a sequence-specific fashion. Most of these sites are mainly tetra-coordinated and contain thiolate ligands (two to four). Indeed, the presence of thiolate ligands is the trademark of structural zinc sites. Accordingly, the presence of sulfur atoms around the zinc in Fur is more consistent with a structural role than a catalytic one.

Fur has to be added to the long list of zinc-containing proteins that interact with DNA, even if there is no homology with zinc finger motif sequences. The identification of the thiolate ligands in the sequence is under progress. The fact that mutation of cysteines 92 and 95 in serines (*1*) causes the loss of activity suggests that these two amino acids can be involved in the zinc ligation. Indeed preliminary results from mass spectrometry/chemical modification experiments support this hypothesis (unpublished experiments). Further investigation has to be done in order to check whether the zinc atom is involved in the dimerization of the Fur protein and in its activity. Up to now, we just know that apoFur (containing Zn) is not active but becomes active upon Co^{2+} or Mn^{2+} incorporation.

In conclusion, this work presents the first structural characterization of the new zinc site found in the Fur protein from *Escherichia coli*. This site is mononuclear with a tetrahedral geometry. The chemical environment is constituted of two sulfur and two light (N/O) atoms. We propose that the two sulfur ligands are the cysteines 92 and 95 known to be essential for the activity. The EXAFS data strongly suggest, in CoFur at least, the presence of one imidazole around the zinc. Cobalt incorporation in apoFur appears to induce a slight distortion of the zinc site without change of the zinc ligands. Altogether the data suggest a structural role for this zinc site in Fur. The analysis of metal-substituted Fur at the K edge of every metal (Mn, Fe, Co) is under progress.

ACKNOWLEDGMENT

We are indebted to G. Sarret (Université Joseph Fourier, Grenoble) and I. Artaud (Université René Descartes, Paris) for the kind gift of the model compounds and to H.-F. Nolting (EMBL Outstation, Hamburg) for providing us data on XAS studies on model compounds. L. Eybert-Berard (Université Joseph Fourier, Grenoble) and R. Vacher (CEA-Grenoble) are thanked for their help in the design and the building of the sample cells. S. Benazeth and F. Villain at the beamline X13 in LURE and Y. Soldo and the technical staff of the BM32 beamline at the ESRF are thanked for technical guidance.

SUPPORTING INFORMATION AVAILABLE

Graph of the average Zn−S distances as a function of the average Zn−N distances in penta- and hexa-coordinated complexes containing nitrogen and sulfur donor ligands (2 pages). Ordering information is given on any current masthead page.

REFERENCES

1. Coy, M., Doyle, C., Besser, J., and Neilands, J. B. (1994) *BioMetals 7*, 292−298.
2. Braun, V., and Hantke, K. (1991) in *Handbook of microbial iron chelates* (Winkelmann, G., Ed) pp 107−138, CRC Press, Boca Raton.
3. Briat, J. F. (1992) *J. Gen. Microbiol. 138*, 2475−2483.
4. Bagg, A., and Neilands, J. B. (1987) *Biochemistry 26*, 5471−5477.
5. Braun, V., Schäffer, S., Hantke, K., and Tröger, W. Eds. (1990) *Regulation of gene expression by iron. The molecular Basis of bacterial metabolism*, Springer-Verlag, Berlin and Heidelberg.
6. De Lorenzo, V., Wee, S., Herrero, M., and Neilands, J. B. (1987) *J. Bacteriol. 169*, 2624−2630.
7. Coy, M., and Neilands, J. B. (1991) *Biochemistry 30*, 8201−8210.
8. Stojiljkovic, I., and Hantke, K. (1995) *Mol. Gen. Genet. 247*, 199−205.
9. Ochsner, U. A., Vasil, A. I., and Vasil, M. L. (1995) *J. Bacteriol. 177*, 7194−7201.
10. Coy, M. (1995) *Biochem. Biophys. Res. Commun. 212*, 784−792.
11. Saito, T., Wordmald, M. R., and Williams, R. J. P. (1991) *Eur. J. Biochem. 197*, 29−38.
12. Hamed, M. Y., and Neilands, J. B. (1994) *J. Inorg. Biochem. 53*, 235−248.
13. Hamed, M. Y. (1993) *J. Inorg. Biochem. 15*, 193-210.
14. Berg, J. M., and Shi, Y. (1996) *Science 271*, 1081−1085.
15. Michaud-Soret, I., Adrait, A., Jacquinod, M., Forest, E., Touati, D., and Latour, J.-M. (1997) *FEBS Lett. 413*, 473−476.
16. Blackburn, N. J., Hasnain, S. S., Diakun, G. P., Knowles, P. F., Binsted, N., and Garner, C. D. (1983) *Biochem. J. 213*, 765−768.
17. Hasnain, S. S., Wardell, E. M., Garner, C. D., Schlösser, M., and Beyersmann, D. (1985) *Biochem. J. 230*, 625−633.
18. Eggers-Borkenstein, P., Priggemeyer, S., Krebs, B., Henkel, G., Simonis, U., Pettifer, R. F., Nolting, H.-F., and Hermes, C. (1989) *Eur. J. Biochem. 186*, 667−675.
19. Skinner, B. P. B. (1959) *Econ. Geol. 54*, 1040.
20. Brand, U., Burth, R., and Vahrenkamp, H. (1996) *Inorg. Chem. 35*, 1083−1086.
21. Goedken, V. L., and Christoph, G. G. (1973) *Inorg. Chem. 12*, 2316−2320.
22. Tsagkalidis, W., and Rehder, D. (1996) *J. Biol. Inorg. Chem. 1*, 507−514.
23. Garrett, T. P. J., Guss, J. M., and Freeman, H. C. (1983) *Acta Crystallogr. C39*, 1027−1031.

24. Alsfasser, R., and Vahrenkamp, H. (1993) *Chem. Ber. 126*, 695−701.
25. Lundberg, B. K. S. (1966) *Acta Crystallogr. 21*, 901−909.
26. Tardat, B., and Touati, D. (1993) *Mol. Microbiol. 9*, 53−63.
27. Wee, S., Neilands, J. B., Bittner, M. L., Hemming, B. C., Haymore, B. L., and Seetharam, R. (1988) *Biol. Met. 1*, 62−68.
28. Teo, B. K. (1981) in *EXAFS Spectroscopy; Techniques and Applications* (Teo, B. K., and Joy, D. C., Eds.) pp 13−58, Plenum Press, New York.
29. Aberdam, D. (1997) The program and its guideline file can be found at this Internet address: http://www.esrf.fr/computing/expg/subgroups/theory/xafs/aberdam.html.
30. Rehr, J. J., de Leon, J., Zabinsky, S. I., and Albers, R. C. (1991) *J. Am. Chem. Soc. 113*, 5135−5140.
31. Rehr, J. J., Albers, R. C., and Zabinsky, S. I. (1992) *Phys. Rev. Lett. 69*, 3397−3400.
32. Landro, J. A., Schmidt, E., Schimmel, P., Tierney, D. L., and Penner-Hahn, J. E. (1994) *Biochemistry 33*, 14213−14220.
33. Durham, P. J. (1988) in *X-Ray Absorption, Principles, applications, techniques of EXAFS, SEXAFS and XANES* (Koningsberger, D. C., and Prins, R., Eds) p 53, John Wiley & Sons, New York.
34. Diakun, G. P., Fairall, L., and Klug, A. (1986) *Nature 324*, 698−699.
35. Strange, R. W., Blackburn, N. J., Knowles, P. F., and Hasnain, S. S. (1987) *J. Am. Chem. Soc. 109*, 7157−7162.
36. Dauter, Z., Wilson, K. S., Sieker, L. C., Moulis, J.-M., and Meyer, J. (1996) *Proc. Natl. Acad. Sci. U.S.A. 93*, 8836−8840.
37. Scott, R. A., and Eidsness, M. K. (1988) *Comments Inorg. Chem. 7*, 235−278.
38. Wang, X., Randall, C. R., True, A. E., and Que, L., Jr. (1996) *Biochemistry 35*, 13946−13954.
39. Gonzales, J. C., Peariso, K., Penner-Hahn, J. E., and Matthews, R. G. (1996) *Biochemistry 35*, 12228−12234.
40. Holm, R. H., Kennepohl, P., and Solomon, E. I. (1996) *Chem. Rev. 96*, 2239−2314.
41. Vallee, B. L., and Auld, D. S. (1993) *Acc. Chem. Res. 26*, 543−551.

BI9721344